Miniaturized Magnetic Bead-Actuators for Force-Clamp Spectroscopy-Based Single-Molecule Measurements

L. Feng, H. Torun*
Faculty of Engineering and Environment, Northumbria University, Newcastle upon Tyne, NE1 8ST, UK

* Corresponding author: Hamdi Torun, hamdi.torun@northumbria.ac.uk

Declarations of interest: none

Abstract

Force-clamp spectroscopy can mimic the physiological conditions for the proteins under investigation. In addition, it is a direct way of observing the relationship between bond lifetime and molecular forces. However, traditional force-clamp methods rely on active feedback controllers that can introduce artefacts. In this work, we introduce a new method to enable force-clamp spectroscopy without a need for an active feedback. The method is based on miniaturized magnetic beads offering improved stability. As a case study, we performed force-clamp experiments using biotin-streptavidin molecule pairs with and without active feedback. Our results demonstrate the feasibility of force-clamp experiments without feedback and illustrate the advantages of our method.

Keywords: Atomic force microscopy; Single-Molecule Mechanics; Force-clamp Spectroscopy; Biotin; Streptavidin

1. Introduction

Mechanics and dynamics of inter- and intra-molecular interactions regulated by mechanical stimuli plays a central role in biology. Spatial and temporal information on mechanical interaction forces at single-molecular level elucidates various biomolecular processes such as cell tethering [1][2], antigen binding to antibody [3][4], and protein folding/unfolding [5][6]. In addition, mechanical measurements at single-molecular level on proteins and cells allow extraction of molecular kinetics and affinities, which are important for drug development [7]. In the past few decades, owing to the technological developments, many single-molecule force measurement techniques have been developed and demonstrated for the investigation of a variety of molecules [8]. Among these, atomic force microscopy (AFM) is one of the most common ones due to its versatility and high spatio-temporal resolution. In conventional AFM force spectroscopy experiments, one end of a molecule that is anchored on a cantilever tip is pulled out of a surface functionalized with interacting molecules with a constant speed. The experiment is repeated by varying the cantilever pulling speed and recording the interaction forces. Subsequently, the potential barrier widths and the corresponding natural transition rates over those barriers can be calculated [9][10]. Alternatively, the biomolecular bonds can be loaded by a constant force until the bonds are broken. It is desirable to perform these experiments under constant force conditions without driving the molecules out of contact so that the experiments will be similar to the physiological conditions. The technique is known as force-clamp spectroscopy where the force between molecules are kept constant using analog [11] or digital feedback controllers [12] and the time duration between the instant of force application until the instant of bond rupture is measured.

In conventional AFM systems, large-scale piezoelectrical actuators control the position of the cantilever against the sample stage. This architecture is prone to drift, hence accurate position control over time durations of few tens of seconds to minutes is challenging [13]. This poses a particular challenge for force-clamp experiments where an accurate control of force is required when the bond is loaded. Thus, force-clamp experiments rely on optimized feedback controllers [14]. Moreover, the relatively large positioners induce significant fluid flow that adversely affect the stability and the dynamics due to hydrodynamic drag [15][16]. Another source of limitation is the

presence of a substrate over which the cantilever operates. In this case, the hydrodynamic effect is enhanced, further increasing the drag and limiting the dynamics [17][18].

Previously, we introduced a new method of actuation using magnetic beads as miniaturized actuators for single-molecule experiments without a need for a piezoelectric actuator or a substrate [19] [20]. We use the piezoelectric actuator only for precise positioning and turn it off during data recording. Instead, we actuate magnetic beads using an electromagnet integrated into a custom-built AFM head. We functionalize the beads with biomolecules and actuate them against an AFM cantilever using the electromagnet while recording the interaction forces using conventional AFM optical lever method. The method of magnetic actuation allows us to eliminate the need for coupling the cantilever to a substrate. Breaking large mechanical loop of an AFM system and reducing the size of the actuator down to the size of an individual molecule, the impact of drift and hydrodynamic drag can be significantly minimized.

In this work, we present a new force-clamp setup utilizing magnetic bead actuators and a software-based controller. The magnetic bead actuation method is advantageous for force-clamp experiments as the need for a feedback controller is eliminated. We compare a set of molecular measurement results with and without feedback for discussion. In these experiments, we used commercially available cantilevers, biotin and streptavidin molecules for benchmarking.

2. Results and Discussion

2.1 Experimental Data with Feedback Control

The experimental method is explained in the Materials and Methods section. Fig.1 shows a typical force and current trace when the feedback controller was activated. In this particular example, we set the force acting on the cantilever as 260 pN and activated the feedback controller. This level corresponds to the total force applied on the cantilever due to all the magnetic beads picked up by the cantilever. When a molecular bond breaks, the corresponding magnetic bead is detached from the cantilever, and the total number of beads, thus the force applied on the cantilever, decreases. Consecutively,

the current applied to the electromagnet is increased by the controller to keep the total force constant. The increase in current in the particular case can be observed as a step change in Fig.1. This event corresponds to a change in force with a magnitude of 120 pN on the cantilever.

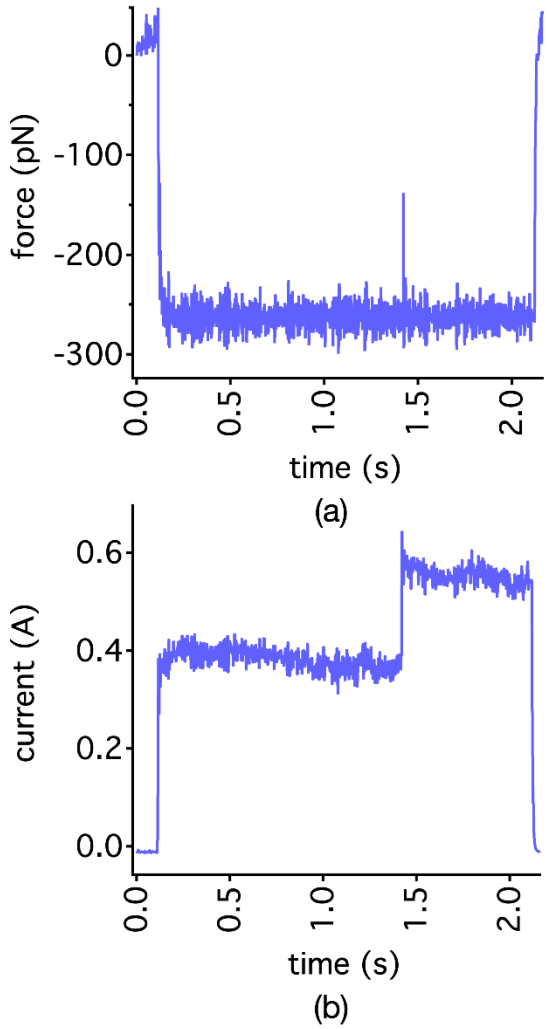

Fig.1 *A typical force trace captured when an event happens while the feedback controller is active at 1.419 s with an unbinding force of 120 pN, resulting in a jump in current by about 0.2 A.*

We repeated this experiment at various clamping forces. We obtained a total of 533 single unbinding events with force magnitudes ranging from 35 pN to 450 pN. We grouped the events by the magnitude of unbinding force to generate force spectrum. An example group with force between 45 pN and 60 pN is shown in Fig. 2. We used these

histograms to estimate the lifetime in each group by fitting exponential probability density functions [21]. The mean value of the force for the fitted function is estimated as 53 pN, corresponding an expected lifetime of 0.261 s with 95% confidential interval (0.211 s, 0.329 s).

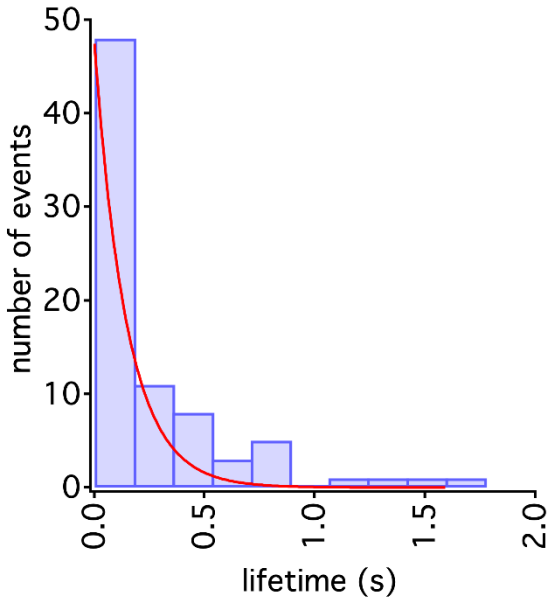

Fig.2. *Histogram of lifetimes measured with a clamping force ranging from 45 pN to 60 pN when feedback controller is on. The mean value of the force is estimated as 53 pN corresponding to an expected lifetime of 0.261 s.*

We analyzed all the force histograms to map the lifetime as a function of clamping force. Fig. 3 shows the natural logarithm of off-rate (reciprocal of lifetime) as a function of force. The collected data indicate the presence of two energy barriers, which have been consistently observed for biotin/streptavidin bonds within our experimental range [22]. We estimated the Bell-Evans' parameters (x_β and K^0 as summarized in Materials and Methods section) as shown in Table 1. Table 1 shows these parameters within one standard deviation.

	Force Range (pN)	K^0 (1/s)	x_β (nm)

Region 1	0-100	1.215±0.128	0.091±0.006
Region 2	100-450	10.202±7.010	0.015±0.011

Table 1. *Estimation of Bell-Evans' parameters derived from fitting the data in two force regions from experiments with feedback controller activated.*

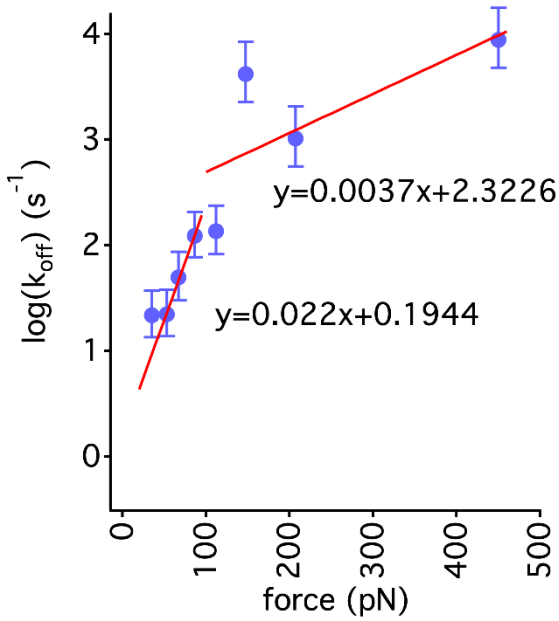

Fig.3 *The variation of off-rate as a function of clamping force when the feedback controller is activated. The presence of two distinct energy barriers is obvious.*

2.2 Experimental Data without any Feedback Control

The current applied on the magnetic coil of the electromagnet determines the strength and gradient of the magnetic field on the cantilever. So, the force applied on the magnetic beads at a fixed location can be kept constant with constant current applied on the coil. We take advantage of this actuation system and have performed force-clamp experiments without any feedback control. The moving structure in this architecture is miniaturized beads while relatively large cantilever is kept stationary. Thus, the drift in the system is significantly minimized. In the case of a molecular bond breakage, the total force on the cantilever suddenly decreases, resulting in a jump on the force trace. An example is shown in Fig.4. Here, the current applied to the coil was kept constant

for 2.5 s while the force trace was recorded. An unbinding event happens at 0.306 s with an unbinding force of 102 pN. No other event was observed until the end of the duration of force application.

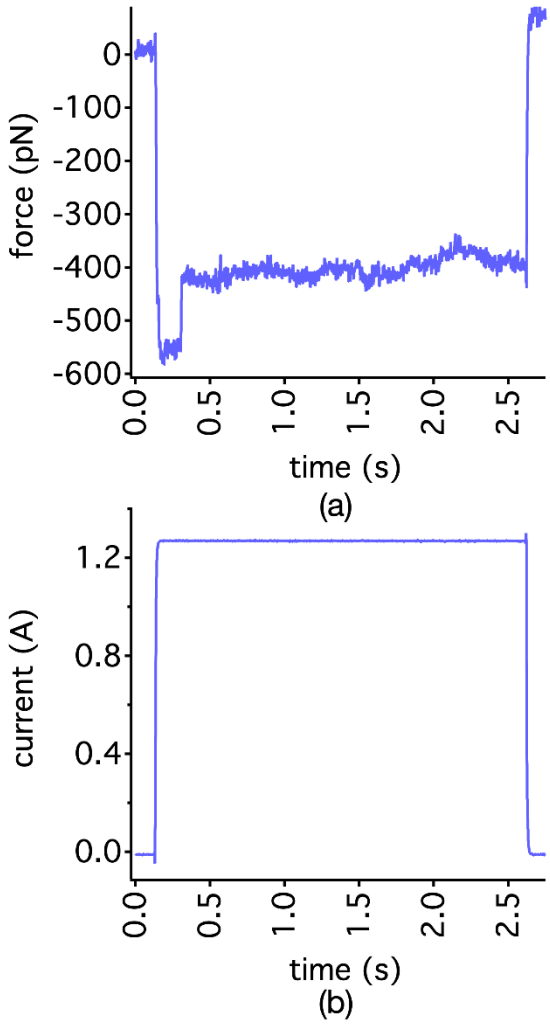

Fig.4 *A typical force trace captured while the feedback controller is tuned off, (a) an event happens at 0.306 s with an unbinding force of 102 pN. (b) the actuation current of 1.3 A starts at 0.133 s then is switched off at 2.621 s.*

Using this approach, we recorded a total of 481 events. The levels of unbinding forces ranging from 32 pN to 304 pN. Similar to the previous case where the feedback controller was active, we grouped the specific events by force levels. Then, we generated histograms of the lifetimes in each group, and fitted exponential probability density functions. An example histogram for unbinding force ranging from 40 pN to 55

pN is shown in Fig.5. The mean value of the force is estimated as 47 pN, corresponding to an expected lifetime of 0.394 s with 95% confidential interval (0.316 s 0.507 s).

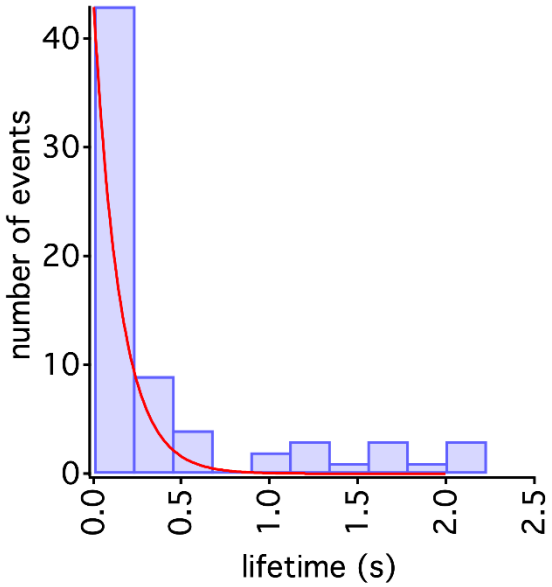

Fig.5. *Histogram of lifetimes measured with a clamping force ranging from 40 pN to 55 pN. The mean value of the force is estimated as 47 pN corresponding to an expected lifetime of 0.394 s.*

Combining all the information from histograms, we obtained the relationship between the off-rate and the clamping force as shown in Fig.6. Similar to the previous case, and consistent with the literature [22], we observed two energy barriers.

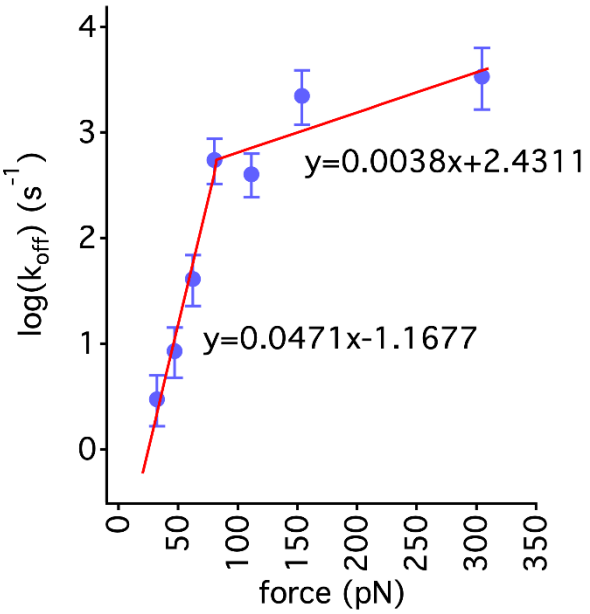

Fig.6 *The variation of off-rate as a function of clamping force when the feedback controller is turned off.*

We estimated the Bell-Evans' parameters using equation 2. Table 2 shows the values for the zero force off-rate and the energy barrier width within one standard deviation.

	Force Range (pN)	K^0 (1/s)	x_β (nm)
Region 1	0-100	0.311±0.093	0.195±0.021
Region 2	100-350	11.373±3.590	0.016±0.007

Table 2. *Estimation of Bell-Evans' parameters derived from fitting the data in two force regions from experiments without using any feedback control.*

2.3 Control experiments

We observed the probability of specific events at 30% during our experiments. The probability of specific events at 30% allows us to resolve the interactions at single bead level. Then, we performed control experiments by saturating biotin on the cantilever with excess streptavidin. The probability of the specific events reduced down to 1%. The significant reduction in specific events indicate the validity of our experimental

protocol for the measurement of molecular pairs.

3. Discussion

We have used an optimized feedback controller with tuned PID parameters. Even if the controller is optimized, the system dynamics depend on the characteristics of the controller in addition to the hardware of the setup. As a comparison, for the case when the feedback is OFF, the system dynamics mainly depend on characteristics of the electromagnet and the cantilever, therefore are less varied. The difference is reflected as a more scattered dataset for the case with activated feedback, especially near the clamping force of 100 pN (see Fig. 7(a)). Since there are variations on the rise times between two cases, the starting time for the calculation of lifetime is chosen as the moment when the actuator is activated. The selection of starting time does not affect the estimation of off-rate as discussed in literature [23]. However, the variations in the rise time may induce errors due to the differences in pulling speed.

The scatter plot in Fig.7 (b) shows the off-rate as a function of clamping force for both feedback ON and OFF cases. The distributions of lifetime for each force level in both cases are very similar, which demonstrates that it is possible to conduct force-clamp experiments without using a feedback system using our method. Indeed, the feedback on case results in a more scattered dataset as it is apparent in Fig. 7(b).

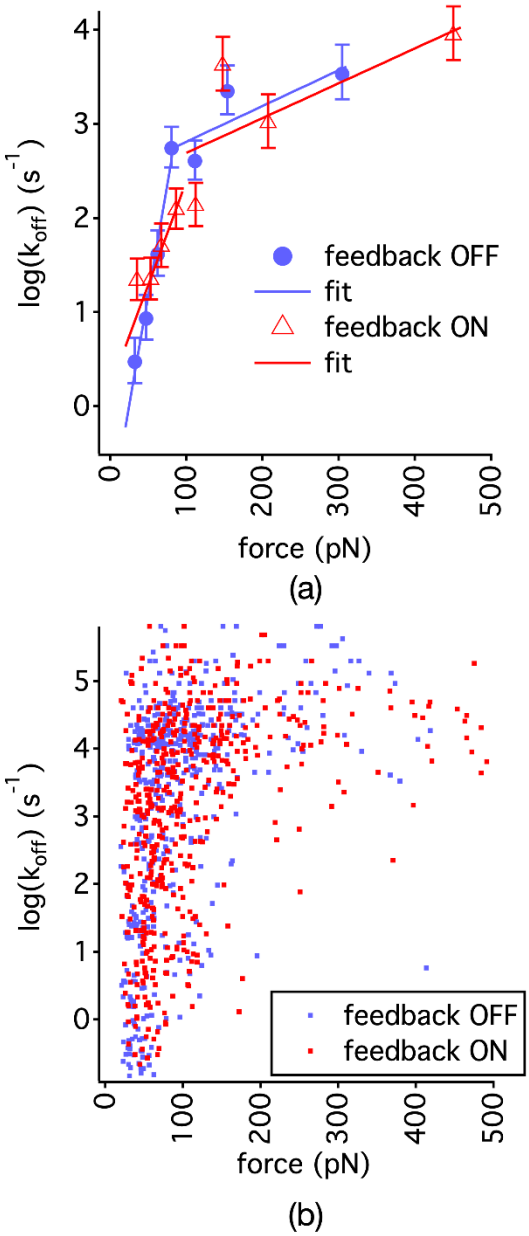

Fig.7. *The comparison of off-rate as a function of clamping force for conditions when feedback controller is on and off. (a) the statistical results and fittings; (b) the first rupture events.*

Multiple events can appear in a single force trace as multiple beads may bind to the cantilever during the contact period. We identified possible estimation errors except for the first events in those multiple even cases. For the feedback ON case, the total force applied on the beads attached on cantilever is constant. When one of the beads falls off from the cantilever, the total force applied on the cantilever reduces. To keep the total force constant, the current will increase in the next controller loop due the error

compensation algorithm of the feedback controller, therefore, the force applied on each bead will increase in a stepwise manner. So, the estimated lifetime for only the first bead will be for a constant force. The subsequent ones will experience increasing forces, while the lifetime will be assessed at the time of rupture. So, the lifetime will be overestimated. In our analysis, we only considered the first unbinding event in a force trace to eliminate this error.

Similarly, in force-clamp without feedback case, the current applied on the magnetic coil is always constant. When a bead falls off from the cantilever, the total force on the cantilever will reduce. Since the actuation current remains constant, the distance between the beads and magnetic coils will increase. So, the remaining beads will experience reduced force. Therefore, the beads except the first one, will experience stepwise decreased force. Thus, lifetimes of the beads, except for the first one, will be underestimated. In our analysis, similar to the previous case, we only considered the first unbinding event in a force trace. The number of events on a single trace can be controlled by varying the density of beads on the surface.

4. Conclusion

We used stationary cantilevers as force sensors and miniaturized magnetic beads as actuators in our customized AFM system. We used a digital controller implemented on LabView to perform force clamp experiment with biotin-streptavidin molecule pair in both feedback ON and OFF methods. We derived the energy landscapes of the molecule pair with Bell-Evans model from the experiment data in both methods, the results are in agreement with previous studies. The distribution of lifetime in each force level are very close in both feedback ON and OFF methods, indicating that it's possible to perform force clamp experiment without using a feedback system in our AFM system.

5. Materials and Method

5.1 The AFM Setup

The customized AFM system consists of a 3D printed head and a sample stage which is integrated with electromagnetic manipulator system. The details of design,

realization, and characterization of the system are explained in our previous work [19]. The software-based controller and user interface are implemented in LabView on a PC operating on a Windows platform. The AFM setup including its controller is schematically shown in Fig.8. The switch to the amplifier of the electromagnet determines the mode of the operation. During the feedback ON case, the input to the electromagnet is controlled using the software-based controller. On the other hand, a constant set force level is fed to the input of the amplifier during feedback OFF case.

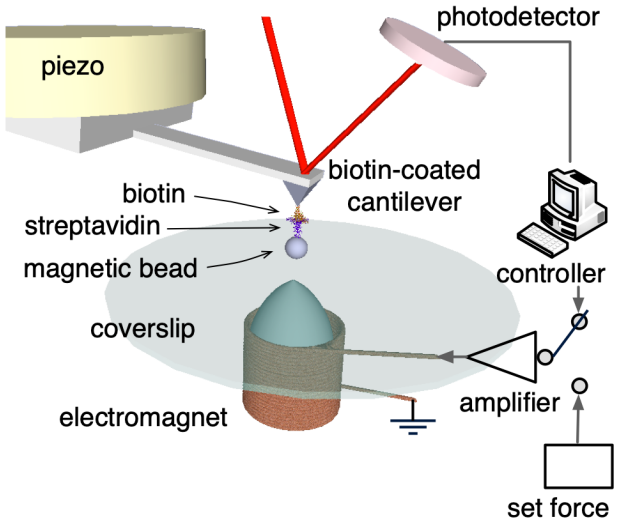

Fig.8. *Schematic overview of the AFM setup. The input of the electromagnet is either controlled using the software-based controller during feedback ON case or it is driven with a constant set force input during feedback OFF case.*

In a typical force-clamp spectroscopy experiment, molecule-A is functionalized on a cantilever and molecule-B is decorated on magnetic beads. The cantilever is first aligned with the tip of the electromagnet beneath a substrate using micromanipulators. Then, the cantilever is brought into contact with the substrate using a piezoactuator attached to it. Magnetic beads are laying on the substrate. The electromagnet is turned on for a few milliseconds to guide the beads towards the tip of the cantilever, facilitating molecular bond formation. After the electromagnet is turned off, the cantilever is brought up to its original resting position using the piezoactuator. Subsequently, the piezoactuator is turned off, and the cantilever is settled for the experiment. Finally, the electromagnet is driven using the controller to pull the magnetic beads towards the sample stage. This operation cycle is a single routine in our system, and we repeat this routine typically several thousand times is a single experiment.

5.2 The Controller

The electromagnet is programmed to precisely control the force on the magnetic beads on demand using a software-based controller implemented on a PXI embedded hardware (NI PXI-8102, National Instruments, TX, USA) operated in LabView environment.

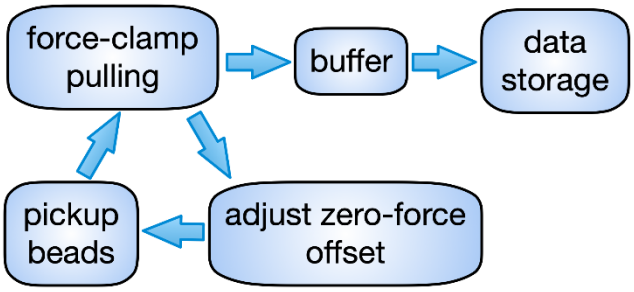

Fig.9. *Block diagram of the software controller.*

The diagram of the controller is shown in Fig.9. State machine approach is used to switch sequentially among three function states: Pick up beads, Force-clamp pulling and Adjust zero force offset, in a cycle. Producer consumer structure is used in the Force-clamp state, where the controller for the actuator, with or without feedback, is run in a timed loop using the internal clock provided by the data acquisition hardware. The feedback controller was implemented with the discrete-time velocity PID algorithm.

Acquired data are first pushed to the buffer in queue then recorded into files through a lower priority loop. In this way, the timing of the controller is independent from the data recording, and controlled by the hardware clock. The controller loop rate is 1 kHz. We characterized the 0-to-100% rise time limited by the dynamics of the electromagnet as 15 ms. We optimized the parameters of the PID controller in the beginning of each experiment by observing the step response of the system. Then, we tuned the feedback parameters in real time, if required. Zero-force level is updated in each routine, therefore it is possible to run the routines and record data autonomously for a few hours

once the sample is prepared and setup is well aligned.

5.3 Data Analysis

We operated the system with and without feedback in a single experiment session and collected data at the same conditions to reduce systematic errors and biases. Only the first rupture event in each data curve were taken into account for statistical analysis. The unbinding events before the setpoint is reached were discarded. The starting instances for the measurements of lifetime are considered as the instant when we observed the cantilever response to the electromagnet.

The data were grouped by force within the vicinity, then in each group, the lifetimes were fitted with exponential fit. The force in each group was taken as the mean of all the data.

With the lifetime and force from all the groups, the data then were fitted using Bell-Evans model, to derive the energy barriers x_β and zero force off-rate K^0 [24]. Here K_{off} is the reciprocal of lifetime, K^0 is the zero force off-rate, f is the force of the molecular bond, x_β is the energy barrier width, K_b is the Boltzmann constant, T is the environment temperature in Kelvin.

$$K_{off} = K^0 \exp\left(\frac{f x_\beta}{K_b T}\right) \tag{1}$$

$$\log\left(K_{off}\right) = \log(K^0) + f * \left(\frac{x_\beta}{K_b T}\right) \tag{2}$$

5.4 Molecules and Consumables.

Commercially available biotin-coated cantilevers (CT.BIO, Novascan, Ames IA USA) and streptavidin functionalized magnetic beads with 2.8um diameter (Dynabeads, M-280 Streptavidin, ThermoFisher Scientific) were used in all our experiments. The sample preparation, calibration and alignment methods were the same as in our previous work [19][20]. The number of events in a single force curve was adjusted by varying the density of beads on the sample stage. The clamping force was kept over a duration

of 2 s, which is long enough for the unbinding events. Bonds with a lifetime longer than 2 s are rare for the selected molecular pairs.

Acknowledgment

Authors would like to acknowledge funding from the EC (ICT FET-Open) under the MANAQA Project, Grant no. 296679.

References

[1] Sun M, Graham J S, Hegedüs B, et al. Multiple membrane tethers probed by atomic force microscopy[J]. biophysical journal, 2005, 89(6): 4320-4329. https://doi.org/10.1529/biophysj.104.058180

[2] Puech P H, Poole K, Knebel D, et al. A new technical approach to quantify cell–cell adhesion forces by AFM[J]. Ultramicroscopy, 2006, 106(8-9): 637-644. https://doi.org/10.1016/j.ultramic.2005.08.003

[3] Dammer U, Hegner M, Anselmetti D, et al. Specific antigen/antibody interactions measured by force microscopy[J]. Biophysical journal, 1996, 70(5): 2437-2441. https://doi.org/10.1016/S0006-3495(96)79814-4

[4] Wang C, Hu R, Morrissey J J, et al. Single Molecule Force Spectroscopy to Compare Natural versus Artificial Antibody–Antigen Interaction[J]. Small, 2017, 13(19): 1604255. https://doi.org/10.1002/smll.201604255

[5] Thompson J B, Hansma H G, Hansma P K, et al. The backbone conformational entropy of protein folding: experimental measures from atomic force microscopy[J]. Journal of Molecular biology, 2002, 322(3): 645-652. https://doi.org/10.1016/S0022-2836(02)00801-X

[6] Puchner E M, Gaub H E. Force and function: probing proteins with AFM-based force spectroscopy[J]. Current opinion in structural biology, 2009, 19(5): 605-614. https://doi.org/10.1016/j.sbi.2009.09.005

[7] Teague S J. Implications of protein flexibility for drug discovery[J]. Nature reviews Drug discovery, 2003, 2(7): 527. https://doi.org/10.1038/nrd1129

[8] Neuman K C, Nagy A. Single-molecule force spectroscopy: optical tweezers, magnetic tweezers and atomic force microscopy[J]. Nature methods, 2008, 5(6):

491. https://doi.org/10.1038/nmeth.1218

[9] Alsteens D, Pfreundschuh M, Zhang C, et al. Imaging G protein–coupled receptors while quantifying their ligand-binding free-energy landscape[J]. Nature methods, 2015, 12(9): 845. https://doi.org/10.1038/nmeth.3479

[10] Pfreundschuh M, Alsteens D, Wieneke R, et al. Identifying and quantifying two ligand-binding sites while imaging native human membrane receptors by AFM[J]. Nature communications, 2015, 6: 8857. https://doi.org/10.1038/ncomms9857

[11] Garcia-Manyes S, Brujić J, Badilla C L, et al. Force-clamp spectroscopy of single-protein monomers reveals the individual unfolding and folding pathways of I27 and ubiquitin[J]. Biophysical journal, 2007, 93(7): 2436-2446. https://doi.org/10.1529/biophysj.107.104422

[12] Bippes C A, Janovjak H, Kedrov A, et al. Digital force-feedback for protein unfolding experiments using atomic force microscopy[J]. Nanotechnology, 2006, 18(4): 044022. https://doi.org/10.1088/0957-4484/18/4/044022

[13] Ricci D, Braga P C. Recognizing and avoiding artifacts in AFM imaging[M]. Atomic Force Microscopy. Humana Press, 2004: 25-37. https://doi.org/10.1007/978-1-61779-105-5_3

[14] Oberhauser A F, Hansma P K, Carrion-Vazquez M, et al. Stepwise unfolding of titin under force-clamp atomic force microscopy[J]. Proceedings of the National Academy of Sciences, 2001, 98(2): 468-472. https://doi.org/10.1073/pnas.98.2.468

[15] Alcaraz J, Buscemi L, Puig-de-Morales M, et al. Correction of microrheological measurements of soft samples with atomic force microscopy for the hydrodynamic drag on the cantilever[J]. Langmuir, 2002, 18(3): 716-721. https://doi.org/10.1021/la0110850

[16] Janovjak H, Struckmeier J, Müller D J. Hydrodynamic effects in fast AFM single-molecule force measurements[J]. European Biophysics Journal, 2005, 34(1): 91-96. https://doi.org/10.1007/s00249-004-0430-3

[17] Craig V S J, Neto C. In situ calibration of colloid probe cantilevers in force microscopy: hydrodynamic drag on a sphere approaching a wall[J]. Langmuir, 2001, 17(19): 6018-6022. https://doi.org/10.1021/la010424m

[18] Tung R C, Jana A, Raman A. Hydrodynamic loading of microcantilevers oscillating near rigid walls[J]. Journal of Applied Physics, 2008, 104(11): 114905. https://doi.org/10.1063/1.4913602

[19] Sevim S, Shamsudhin N, Ozer S, et al. An Atomic Force Microscope with Dual

Actuation Capability for Biomolecular Experiments[J]. Scientific reports, 2016, 6: 27567. https://doi.org/10.1038/srep27567

[20] Sevim S, Ozer S, Feng L, et al. Dually actuated atomic force microscope with miniaturized magnetic bead-actuators for single-molecule force measurements[J]. Nanoscale Horizons, 2016, 1(6): 488-495. https://doi.org/10.1039/C6NH00134C

[21] Popa I, Kosuri P, Alegre-Cebollada J, et al. Force dependency of biochemical reactions measured by single-molecule force-clamp spectroscopy[J]. Nature protocols, 2013, 8(7): 1261. https://doi.org/10.1038/nprot.2013.056

[22] Teulon J M, Delcuze Y, Odorico M, et al. Single and multiple bonds in (strept) avidin–biotin interactions[J]. Journal of Molecular Recognition, 2011, 24(3): 490-502. https://doi.org/10.1002/jmr.1109

[23] Cao Y, Li H. Single-molecule force-clamp spectroscopy: dwell time analysis and practical considerations[J]. Langmuir, 2010, 27(4): 1440-1447. https://doi.org/10.1021/la104130n

[24] Lee C K, Wang Y M, Huang L S, et al. Atomic force microscopy: determination of unbinding force, off rate and energy barrier for protein–ligand interaction[J]. Micron, 2007, 38(5): 446-461. https://doi.org/10.1016/j.micron.2006.06.014